

Basic considerations on broken-symmetry states of organic superconductors

C. Bourbonnais

Centre de Recherche sur les Propriétés Électroniques de Matériaux Avancés, Département de Physique,
Université de Sherbrooke, Sherbrooke, Québec, Canada J1K 2R1

In this brief account, we shall review the different mechanisms giving rise to itinerant and localized antiferromagnetism in quasi-one-dimensional organic conductors: the Bechgaard salts and their sulfur analogs. We will then focus on the problem of spin correlations and their impact on the pairing mechanism for organic superconductivity.

I. INTRODUCTION

The discovery of superconductivity twenty years ago by Jérôme *et al.* [1], in the charge transfer salt $(\text{TMTSF})_2\text{PF}_6$ was not only remarkable for superconductivity itself, but also showed that superconductivity in a quasi-one-dimensional electronic material could emerge from a competition with antiferromagnetism under pressure. This unusual interplay between magnetism and superconductivity turned out to be a common characteristic of other members of the Bechgaard salts series $(\text{TMTSF})_2\text{X}$ and their sulfur analogs: the Fabre salts $(\text{TMTTF})_2\text{X}$ [2]. Similar competition of ground states was also found in other low-dimensional many-electron systems such as the layered organic superconductors and high- T_c cuprates [3–5].

Antiferromagnetism and superconductivity are therefore closely related in these systems and can no longer be considered as completely blind to each other. In spite of the considerable interest bestowed on this issue over the last twenty years, their connection remains so far largely unexplained and stands as one of the most important challenges of the physics of low-dimensional organic superconductors.

II. ANTIFERROMAGNETISM

By sharing a common boundary with superconductivity and being present in a relatively large domain of the normal phase in the form of short range correlations, antiferromagnetism has become a dominant feature of the whole phase diagram of $(\text{TM})_2\text{X}$ (Figure 1). Thus attempts to unravel the origin of superconductivity in the Bechgaard salts and their sulfur analogs must inevitably go through a proper understanding of the mechanisms leading to magnetism in these electronic materials.

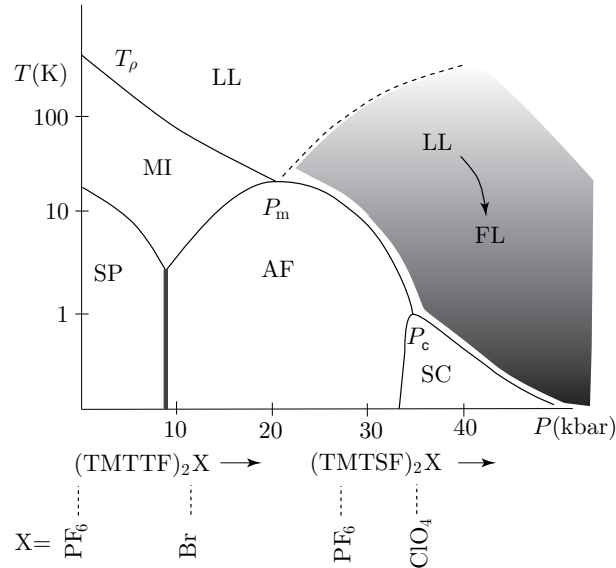


FIG. 1. The generic phase diagram of the Bechgaard and Fabre salts $[(\text{TM})_2\text{X}]$ as a function of pressure or anion X substitution, after ref. [6].

A. The nesting mechanism: success and limitations

The observation of itinerant antiferromagnetism in $(\text{TMTSF})_2\text{X}$ indicated from the outset that electron-electron Coulomb repulsion, not electron-phonon interaction, would play a more important part in the instability of the metallic state. However, it should be stressed that repulsive interactions alone, only lead in a metal to uniform, (i.e., ferromagnetic) spin correlations. These enhance the magnetic spin susceptibility with respect to the Pauli or noninteracting band limit – an effect that is confirmed by experiments [6]. Adopting a weak coupling picture for electrons, the mechanism of density-wave formation, called nesting, originates from an instability of the Fermi surface. For a quasi-one-dimensional metal, constant energy electron and hole states located on opposite sides ($\sim \pm \mathbf{k}_F$) of the open Fermi surface can be connected or nested on one another. This is expressed by the following relation for the energy of one-electron states

$$\epsilon_{\pm}(\mathbf{k}) = -\epsilon_{\mp}(\mathbf{k} + \mathbf{Q}_0) + \delta\epsilon_0, \quad (1)$$

where $\mathbf{Q}_0 = (2k_F^0, \mathbf{q}_\perp^0)$ is called the nesting vector of the Fermi surface, with $2k_F^0$ corresponding to the nesting vector of the single chain. Here, $\delta\epsilon_0$ stands as corrections that parametrize deviations from perfect nesting.

For perfect nesting, the electron gas develops a singular logarithmic response to density-wave formation at wavevector \mathbf{Q}_0 , as shown by the expression of the free electron gas susceptibility at \mathbf{Q}_0 :

$$\begin{aligned}\chi_0(\mathbf{Q}_0, \omega) &= \frac{2}{LN_{\perp}} \sum_{\mathbf{k}} \frac{n[\epsilon_+(\mathbf{k})] - n[\epsilon_-(\mathbf{k} + \mathbf{Q}_0)]}{\epsilon_+(\mathbf{k}) - \epsilon_-(\mathbf{k} + \mathbf{Q}_0) - \omega + i0^+} \\ &= N(E_F) \ln \frac{E_0}{T} \quad (\delta\epsilon_0 = 0, \omega = 0),\end{aligned}\quad (2)$$

where the last expression follows in the static limit. Here, E_0 is a cut-off energy and $N(E_F)$ is the noninteracting electron density of states at the Fermi level. Repulsive interaction that scatters two electrons at $\pm\mathbf{k}_F$ gives rise to an attraction between electron and hole separated by \mathbf{Q}_0 , which according to (2) will be magnified as function of temperature and can become singular. In leading (ladder) order, this is well known to yield the simple pole singularity of the total forward scattering amplitude, namely

$$\Gamma(\mathbf{Q}_0, \omega) = \frac{g^*}{1 - g^* \chi_0(\mathbf{Q}_0, \omega)}, \quad (3)$$

where g^* is an effective coupling defined at the scale E_0 (for simplicity, we have dropped the contribution of umklapp scattering). The characteristic temperature T_{SDW} signaling an SDW instability of the normal state then follows the pattern of the BCS mechanism for superconductivity. The temperature at which bound electron-hole pairs condense is determined by the condition $1 = g^* \chi_0(\mathbf{Q}_0, T_{SDW})$, corresponding to the simple pole singularity of Γ in the static limit, and this yields

$$T_{SDW} \sim t_{\perp}^* e^{-1/N(E_F)g^*}. \quad (4)$$

Within this weak-coupling picture of the SDW transition, the identification of the cut-off E_0 in (2) with an effective – renormalized – value of the interchain hopping amplitude t_{\perp}^* ($< t_{\perp}$) takes on particular significance in quasi-one-dimensional systems. It stands as the temperature for crossover towards the one-dimensional metallic state. It imposes a mechanical limitation of the above approach to the temperature domain $T < t_{\perp}^*$, where the curvature of the Fermi surface and in turn the transverse momentum of electrons is coherent in the quantum-mechanical sense. Otherwise, for $T > t_{\perp}^*$, thermal fluctuations reduce nesting properties to be essentially longitudinal or one-dimensional in character, a configuration that introduces interference between electron-hole and electron-electron (Cooper) pairings. An immediate outcome of this interference is to invalidate the ladder summation in (3), which assumes that electron-hole pairing can be singled out in perturbation theory. The metallic state then turns out to be no longer a Fermi liquid but rather a Luttinger liquid. For repulsive interactions, however, SDW correlations are singular over the whole 1D temperature domain. According to the one-dimensional theory,

their amplitude is governed by a power law increase of the susceptibility at wavevector $2k_F^0$:

$$\chi_0(2k_F^0, T) \sim T^{-\gamma}, \quad (5)$$

where γ is an exponent that depends on the strength of electron-electron interaction.

The application of pressure modifies electron band energy in such a way that nesting deviations ($\delta\epsilon_0$) increase and cut off the logarithmic singularity following the approximate expression

$$\chi(\mathbf{Q}_0, T) \approx N(E_F) \ln \frac{t_{\perp}^*}{\sqrt{\delta\epsilon_0^2 + T^2}}. \quad (6)$$

As pressure increases, the SDW critical temperature derived from (3) is then progressively shifted down to lower temperature and ultimately vanishes whenever $\delta\epsilon_0(P)$ exceeds a certain threshold ($\sim T_{SDW}$) [7]. The rapid suppression of T_{SDW} thus obtained under pressure squares relatively well with observation made close to P_{c2} (Figure 1). The involvement of nesting as a mechanism of stability of itinerant antiferromagnetism is however most substantiated by its remarkable ability to account for the restoration of a cascade of SDW states induced by a magnetic field above P_{c2} [8,9]. When a magnetic field is applied along the less conducting axis, open orbits are produced which confine electron motion preferentially along the chains where full, but quantized, nesting properties are found to be restored. In this way, the logarithmic singularity in $\chi_0(\mathbf{Q}_N, T, H)$ is recovered for a given set of discrete nesting wavevectors \mathbf{Q}_N and shows a particular variation with field. Following (3), a characteristic hierarchy or cascade of $T_{SDW}(N)$ is found with quite remarkable consequences on physical properties. For example, the quantization of Hall resistance has received sound experimental support [10,11].

In spite of this apparent success of the BCS mechanism to explain long-range SDW order, difficulties arise when one tries to tackle from the same standpoint the properties of the metallic state. One of the main defects of the approach, as it is formulated, lies in the assumption that all electron excitations of the normal state can be described within the Fermi liquid framework, which is not corroborated by most experiments. In a Fermi liquid for example, electron correlation effects are essentially absent of the scene from $T \sim t_{\perp}^*$ down to the close vicinity of T_{SDW} , where the onset of critical fluctuations ultimately limits the validity of the quasi-particle picture. Thus in the BCS description, the temperature interval ΔT_{fl} for SDW fluctuation effects, albeit increased by spatial anisotropy, is small compared to T_{SDW} and a reduction of T_{SDW} is concomitant to a reduction of ΔT_{fl} , which vanishes with T_{SDW} .

The NMR spin-lattice relaxation rate T_1^{-1} was among the first properties to show the existence in the Bechgaard salts of spin correlations whose amplitude did not

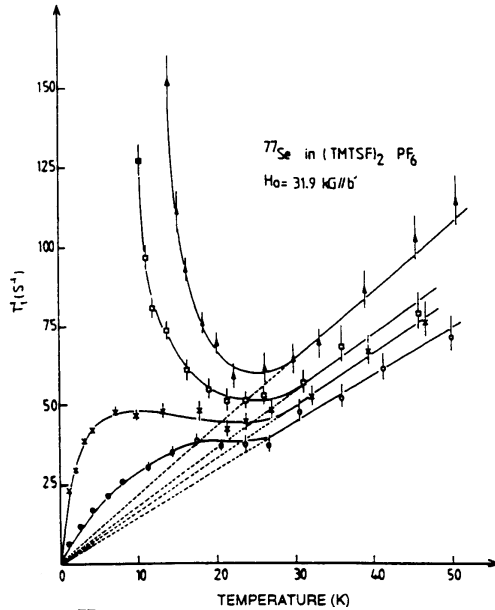


FIG. 2. ^{77}Se NMR relaxation rate as a function of temperature below (1 bar and 5 kbar) and above (8 kbar and 10 kbar) P_c in $(\text{TMTSF})_2\text{PF}_6$, after ref. [12].

agree with the Fermi liquid prediction [12,13]. In this matter, the temperature dependent T_1^{-1} data of Figure 2 obtained for $(\text{TMTSF})_2\text{PF}_6$ are particularly revealing of the importance of antiferromagnetic spin correlations in the normal state near P_c . For pressures above P_c , where the system is no longer in a SDW state but is expected to be a superconductor, a huge enhancement of the relaxation rate persists over a large temperature interval. Given the extent in temperature of the enhancement and its non critical character, it contrasts with the Korringa law behavior $(T_1 T)^{-1} \approx \text{constant}$, that should be found for a weakly interacting Fermi liquid. In view of quite similar effects reported for other members of the series, as well as other experimental signs of correlation effects [6], all this goes to show that antiferromagnetic spin correlations of the normal state of $(\text{TMTSF})_2\text{X}$ differ from those found in a conventional metal.

On the theoretical side, it is worthy of note that it was at first proposed that these non Fermi liquid effects are attributable to a sizeable reduction – or renormalization – of the one-dimensional temperature scale t_\perp^* as a self-consistent effect of correlations themselves [13]. According to this scheme, a reduction of t_\perp^* would widen the temperature domain in which low-dimensional spin correlations lead to a power law increase of enhancement for the relaxation rate $(T_1 T)^{-1} \sim T^{-\gamma}$. This renormalization effect on the kinetics of electrons does solve a number of problems about the normal state but is not beyond creating new paradoxes [14] – in particular concerning the transport properties and field-induced SDW states [15–17]. A central point at issue is the determina-

tion of the actual value taken by this temperature scale and if t_\perp^* rather corresponds to a smooth crossover between the Luttinger and Fermi liquids (Figure 1).

B. The sulfur series and the Mott insulating picture

It is instructive to compare the Bechgaard salts with the $(\text{TMTTF})_2\text{X}$ series of Fabre salts. The members of this series are located on the left of the phase diagram in Figure 1; their study has provided extremely valuable and rather well understood pieces of information about both the nature of correlations and the mechanisms of long-range order in a sector of the phase diagram that stands only few kilobars apart from the Bechgaard salts. At low pressure, the nature of the transition in $(\text{TMTTF})_2\text{X}$ shows qualitative differences with respect to the Bechgaard salts: antiferromagnetism is stabilized from a paramagnetic state that is insulating. The metal to insulator ‘transition’ occurs at a characteristic temperature usually denoted as $T_\rho \sim 10^2$ K (Figure 1), below which electrical transport develops a thermally activated behavior [18]. Since spin degrees of freedom remain unaffected at T_ρ – as shown by the absence of anomaly in the spin susceptibility at that temperature [6] – $(\text{TMTTF})_2\text{X}$ are good examples of Mott insulators below T_ρ [19]. The measured amplitude of the Mott insulating gap $\Delta_\rho \sim 3T_\rho$ even exceeds the transverse bare hopping amplitude t_\perp obtained from band calculations [20]. The carriers can then be considered as confined on organic stacks, while spin excitations are gapless and dominated by one-dimensional physics. The one-dimensional nature of spin correlations associated to the Mott insulating state in $(\text{TMTTF})_2\text{X}$ has received several experimental confirmations [21,22]. As regards to NMR for example, the one-dimensional theory predicts a power law enhancement of $(T_1 T)^{-1} \sim T^{-\gamma}$ at $2k_F^0$ with the exponent $\gamma = 1$ for a 1D Mott system [23,24], a behavior that has indeed been found in the paramagnetic phase of all sulfur compounds studied down to the vicinity of their critical point [22].

In spite of charge confinement along the chains, spin degrees of freedom ultimately deconfine and lead to antiferromagnetic long-range order which is found in the range 5–25 K for $(\text{TMTTF})_2\text{X}$. However, the mechanism by which antiferromagnetic correlations propagate in the transverse direction is here not connected with the Fermi surface. Owing to charge localization, the system is clearly not a Fermi liquid so that the antiferromagnetic transition cannot be driven from Fermi surface effects but rather from the interchain kinetic exchange (superexchange) coupling J_\perp [25,26]. This coupling between spins is in effect not present in the Hamiltonian in the high-energy limit; it is generated through virtual interchain hopping of electrons confined within the coherence length $\xi_\rho \sim v_F/\Delta_\rho$ induced by the Mott gap (Figure 3). The

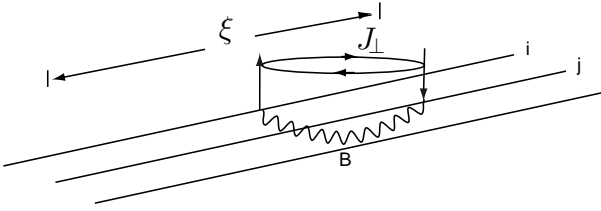


FIG. 3. Interchain kinetic exchange (superexchange) between spins on neighboring chains i and j . In the presence of a Mott gap, the antiferromagnetic exchange takes place over the coherence length $\xi \rightarrow \xi_\rho \sim v_F/\Delta_\rho$ corresponding to the size of bound electron-hole pairs along the chains. The process given in B refers to exchange of spin fluctuations which gives rise to attractive pairing on different chains.

explicit expression for the effective interchain exchange Hamiltonian at the scale $\sim T_\rho$ is known and can be determined by the renormalization group method [27,28]:

$$H_\perp \approx \int dx \sum_{\langle i,j \rangle} J_\perp \mathbf{S}_i(x) \cdot \mathbf{S}_j(x), \quad (7)$$

where

$$J_\perp \approx \frac{\xi_\rho}{a} \frac{t_\perp^{*2}}{\Delta_\rho}. \quad (8)$$

Here t_\perp^* stands as the effective interchain hopping taking place at the energy scale $\sim T_\rho$. J_\perp couples to singular antiferromagnetic correlations along the chains and induces a true transition at finite temperature (in three dimensions). In a very good approximation, the transverse part H_\perp can be treated in molecular-field approximation and 1D correlations exactly, so that the singular part of the total antiferromagnetic susceptibility at the $(2k_F^0, \pi)$ reads

$$\chi(\mathbf{Q}_0, T) = \frac{\chi(2k_F^0, T)}{1 - J_\perp \chi(2k_F^0, T)}, \quad (9)$$

where $\chi(2k_F^0, T)$ is given by the one-dimensional form (5) with $\gamma = 1$. The Néel transition then takes place at

$$T_N \sim \frac{t_\perp^{*2}}{\Delta_\rho}. \quad (10)$$

It follows from this result a characteristic increase of T_N as Δ_ρ or T_ρ decreases under pressure. This feature which comes from a magnification of J_\perp due to the progressive deconfinement of carriers, agrees with observations (cf. Figure 1) [29]. In the case of $(\text{TMTTF})_2\text{Br}$ for example, a relation of the form $T_\rho T_N \approx \text{constant}$ under pressure has been shown to be well satisfied by the data [30].

The drop of T_ρ carries on under pressure until it merges with the critical domain associated with the transition.

This pressure scale, which is denoted as P_m in Figure 1, signals a change of regime of the normal state, which becomes metallic. The insulator to metal crossover marks the onset of charge deconfinement and weaker coupling conditions for the carriers. This is exemplified by a reduction of the enhancement in NMR $(T_1 T)^{-1}$ [22], and the restoration of a transverse plasma edge in optical experiments [31]. Such a change in the strength of electron correlations has a characteristic impact on the pressure profile of T_N under pressure, which presents a maximum at P_m . This feature, which is predicted by microscopic calculations [28], comes essentially from the pressure variation of J_\perp whose magnification in (8), as a result of the increase of ξ_ρ , levels off at the boundary and finally decreases above P_m . It turns out that even in the absence of an insulating behavior, J_\perp remains the main driving mechanism of the transition close to P_m . Its influence grows less and less as one moves away from P_m to finally become coupled to the nesting mechanism whose importance follows the growth of the Fermi liquid component under pressure. As one can see, the question that was previously raised about both the degree of renormalization of t_\perp^* and correlation effects in the normal phase of the Bechgaard salts, is closely related to the extent to which antiferromagnetic exchange is still active for magnetic ordering on the right-hand side of the diagram of Figure 1.

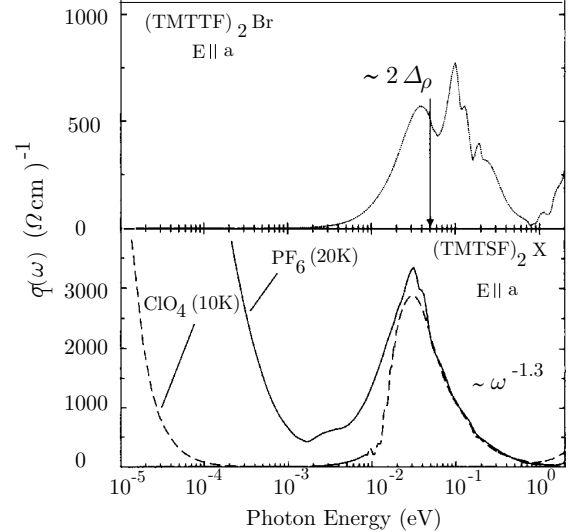


FIG. 4. One-chain optical conductivity of members of $(\text{TM})_2\text{X}$ in the normal phase at low temperature. The arrow indicate the size of (twice) the Mott gap, after [31].

On the theoretical side, this important question has not received a clear answer so far. Nonetheless, it is instructive in this matter to look at experiments giving relevant information about the spectral response of these materials [31,32]. For example, the optical conductivity obtained by Vescoli *et al.* [31] from infrared reflectivity data, are shown in Figure 4 for members of both series

in their normal phase. The results show that the Mott gap, which is the dominant structure in the sulfur compound, remains clearly visible in the Bechgaard salts, yet metallic [33]. The gap structure captures 99% of the spectral weight, whereas the large metallic DC conductivity provided by a narrow frequency mode carries the remaining 1%. These results clearly indicate that the build-up of short-range correlations along the stacks is achieved for strongly coupled electrons. This implies in turn that interchain exchange is likely to be well developed in $(\text{TMTSF})_2\text{X}$.

III. ORGANIC SUPERCONDUCTIVITY

We now examine the impact spin correlations can have on the nature of organic superconductivity. We ground the analysis on the following experimental information: i) as shown by NMR, the normal phase is dominated by antiferromagnetic correlations (Figure 2); ii) the superconducting T_c and T_{SDW} join at P_c , where T_c presents a maximum (Figure 1); iii) there is no lattice softening at $2\mathbf{k}_F$. What should be established at the very outset is that spin correlations in the normal phase lead to an enhancement of electron-electron repulsion. This immediately follows from the expression of the vertex part in (3) close to T_{SDW} . A large increase of the forward scattering between carriers that move in opposite directions yields quite unfavorable conditions for conventional BCS superconductivity [34]. These conditions become even worst when the influence of interchain exchange J_\perp is included in the analysis [27].

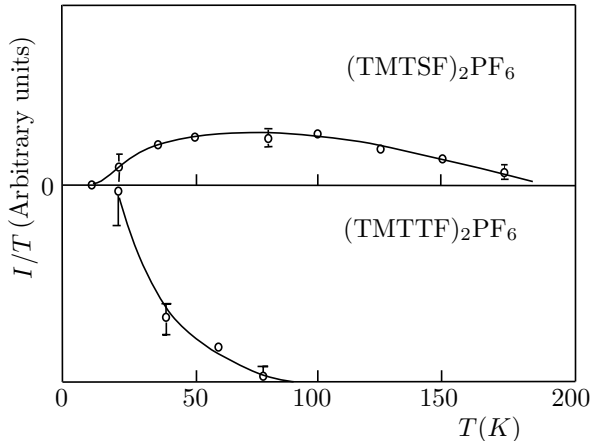


FIG. 5. Temperature dependence of the $2k_F^0$ lattice susceptibility (I/T) as function of temperature in the normal phases of $(\text{TMTSF})_2\text{PF}_6$ (top) and $(\text{TMTTF})_2\text{PF}_6$ (bottom), after [35].

In the traditional BCS scheme for superconductivity, the repulsion between electrons must be completely screened by the attraction produced the exchange of virtual phonons — a screening made possible only below

the Debye temperature θ_D due to retardation. For narrow tight-binding bands in the organics [36], the attraction is strongest for backscattering processes in which $2\mathbf{k}_F$ phonons are exchanged. According to the results of X-ray experiments performed on $(\text{TMTSF})_2\text{X}$, however, the electron-phonon vertex part at this wavevector does not undergo any significant increase in the normal state [35]. As it is indeed seen in the upper-half of Figure 5 for $(\text{TMTSF})_2\text{PF}_6$, the amplitude of the $2k_F^0$ lattice susceptibility — which is directly involved in the strength of the phonon exchange — is weak (a result also found for $(\text{TMTSF})_2\text{ClO}_4$ [35]). On this matter, it is instructive to compare with the sulfur analog compound $(\text{TMTTF})_2\text{PF}_6$ (Figure 5, bottom), for which the electron-phonon vertex part at $2k_F^0$ becomes singular, signaling a lattice instability towards a spin-Peierls distortion (left-hand side of Fig. 1). This instability produces a spin gap that is clearly visible in the temperature dependence of magnetic susceptibility and nuclear relaxation rate [21,37]; these effects are not seen in $(\text{TMTSF})_2\text{X}$ close to P_c . The persistent enhancement of these quantities indicates that interactions are dominantly repulsive, making the traditional phonon-mediated source of pairing essentially inoperant in $(\text{TM})_2\text{X}$. Added to that, it should be stressed that the restoration of the SDW states under magnetic field above P_c gives an additional support of a positive value for g^* in this pressure range.

The above discussion naturally brings us to the question of the nature of pairing mechanism when electrons move in the presence of antiferromagnetic spin correlations. As suggested by Emery [38,34], long-lived antiferromagnetic spin fluctuations of wavevector \mathbf{Q}_0 give rise to an oscillating potential in real space at the corresponding periodicity, to which electrons are coupled. Electrons moving in opposite directions can thus avoid local repulsion and even be attracted to each other if they move on different chains. The attraction being strongest for neighboring chains produces a gap with nodes on the Fermi surface. This mechanism can be seen as the spin-analog of the so-called Kohn-Luttinger mechanism proposed for superconductivity induced by electrons exchanging charge-density excitations — as produced by Friedel oscillations [39].

By virtue of the rather large temperature domain where spin correlations are present (Figure 2), one can expect that the K-L mechanism can emerge relatively deep in the normal phase giving in turn rise to interchain pairing correlations [27,40]. Given the inability of the BCS nesting mechanism to produce spin correlations over a large temperature domain, it cannot alone account for pairing fluctuations far from T_c . But interchain superexchange does. Following the analysis of Ref. [40], singlet interchain pairing correlations dominate when intrachain SDW correlations couple through the interchain superexchange. This is shown for instance by the following expression for the pairing susceptibility in the normal

state:

$$\chi_{i,j}^\perp(T) \sim [1 - J_\perp(T)\chi(T)]^{-3/2}, \quad (11)$$

where $J_\perp(T)$ stands for an effective temperature dependent transverse superexchange. It is worth noting here that no (antisymmetric) interchain *triplet* pairing correlations are found to be induced by SDW fluctuations.

As regards to the critical temperature T_c , some interesting features can be drawn in the framework of the spin-fluctuations exchange mechanism. Adopting the simple picture where a Fermi liquid component exists near P_c – consistently with the suppression of T_{SDW} due to nesting deviations –, the ‘propagator’ of spin fluctuations involved in pairing attraction reads:

$$V(\mathbf{Q}, \omega) = \frac{V_0}{r + \sum_i \xi_{0,i}^2 (Q_i - Q_0)^2 - i\omega/\omega_0}, \quad (12)$$

where $r = [T - T_{SDW}(P)]/T_{SDW}(P)$, $\xi_{0,i}$ is the SDW coherence length in the $i = x, y, z$ directions, and $\omega_0 \sim T_{SDW}$ is a characteristic frequency scale for spin fluctuations. The critical temperature for superconductivity can be calculated within a standard BCS procedure. The result for T_c can be written in the familiar form:

$$T_c \sim \omega_0 e^{-1/\lambda^*}, \quad (13)$$

where in the usual way, ω_0 enters as a cut-off for T_c due to retardation. The effective coupling constant $\lambda^* \propto 1/\kappa$ involves a ‘stiffness’ constant κ ($\kappa \rightarrow 0$ as $r \rightarrow 0$) of the SDW fluctuations. Therefore as one approaches P_c , r becomes small so that λ^* reaches strong coupling but ω_0 remains small. In these conditions, the growth of T_c levels off and reaches a maximum in agreement with the maximum commonly seen at P_c (Figure 1). This can be seen as a limitation of T_c in $(\text{TM})_2\text{X}$, a situation that, bears an obvious resemblance with the limitation of T_c in conventional superconductors, where the increase of T_c reaches a maximum when the elasticity of the lattice becomes too soft and the coupling becomes strong. In the present spin-fluctuation scheme, the maximum T_c would therefore scale with ω_0 . Above P_c , the amplitude of fluctuations decreases (Figure 2), so that T_c is dominated by a reduction of λ^* and therefore becomes a decreasing function of pressure [41].

In conclusion, the existence of spin correlations in $(\text{TM})_2\text{X}$ near the critical pressure for superconductivity indicates that the normal phase precursor to this broken-symmetry state is strongly correlated and would make the conventional electron-phonon mechanism inoperant for the origin of this phase. Interchain superexchange is set to play an important role in these systems not only in the stabilization of long-range magnetic ordering but also as a mechanism that magnifies pairing induced by spin-fluctuation exchange.

Acknowledgements The author thanks D. Jérôme, L. G. Caron, B. Guay and R. Duprat for valuable discussions on several aspects of this brief review. The author would also like to thank D. Sénechal for very useful comments. This work is supported by NSERC of Canada and the Superconductivity program of the Canadian Institute of Advanced Research (CIAR).

-
- [1] D. Jérôme, A. Mazaud, M. Ribault, and K. Bechgaard, J. Phys. (Paris) Lett. **41**, L95 (1980).
- [2] D. Jérôme and H. Schulz, Adv. in Physics **31**, 299 (1982).
- [3] K. Kanoda, Physica C **282-287**, 299 (1997).
- [4] R. H. McKenzie, Comments Cond. Matt. Phys. **18**, 309 (1998).
- [5] S. Lefebvre *et al.*, this volume and to be published.
- [6] C. Bourbonnais and D. Jérôme, in *Advances in Synthetic Metals, Twenty Years of Progress in Science and Technology*, edited by P. Bernier, S. Lefrant, and G. Bidan (Elsevier, New York, 1999), pp. 206–261.
- [7] K. Yamaji, J. Phys. Soc. of Japan **51**, 2787 (1982).
- [8] L. P. Gorkov and A. G. Lebed, J. Phys. (Paris) Lett. **45**, L433 (1984).
- [9] M. Héritier, G. Montambaux, and P. Lederer, J. Phys. (Paris) Lett. **45**, L943 (1984).
- [10] D. Jérôme, in *Organic Conductors: fundamentals and applications*, edited by J.-P. Farges (Dekker, New York, 1994), pp. 405–494.
- [11] P. Chaikin, J. Phys. I (France) **6**, 1875 (1996).
- [12] F. Creuzet *et al.*, Synthetic Metals **19**, 277 (1987).
- [13] C. Bourbonnais *et al.*, J. Phys. (Paris) Lett. **45**, L755 (1984).
- [14] A. Georges, T. Giamarchi, and N. Sandler, preprint cond-mat/0001063 (unpublished).
- [15] G. M. Danner, W. Kang, and P. M. Chaikin, Phys. Rev. Lett. **72**, 3714 (1994).
- [16] J. Moser *et al.*, Eur. Phys. J. B **1**, 39 (1998).
- [17] A. T. Zheleznyak and V. M. Yakovenko, Eur. Phys. J. B **11**, 385 (1999).
- [18] C. Coulon *et al.*, J. Phys. (Paris) **43**, 1059 (1982).
- [19] V. J. Emery, R. Bruinsma, and S. Barisic, Phys. Rev. Lett. **48**, 1039 (1982).
- [20] L. Balicas *et al.*, J. Phys. I (France) **4**, 1539 (1994).
- [21] F. Creuzet *et al.*, Synthetic Metals **19**, 289 (1987).
- [22] P. Wzietek *et al.*, J. Phys. I (France) **3**, 171 (1993).
- [23] C. Bourbonnais, J. Phys. I (France) **3**, 143 (1993).
- [24] V. J. Emery, in *Highly Conducting One-Dimensional Solids*, edited by J. T. Devreese, R. E. Evrard, and V. E. van Doren (Plenum Press, New York, 1979), p. 247.
- [25] S. Brazovskii and Y. Yakovenko, Sov. Phys. JETP **62**, 1340 (1985).
- [26] C. Bourbonnais and L. G. Caron, Physica **143B**, 450 (1986).
- [27] C. Bourbonnais and L. Caron, Europhys. Lett. **5**, 209 (1988).
- [28] C. Bourbonnais, in *Les Houches, Session LVI* (1991),

- Strongly interacting fermions and high- T_c superconductivity*, edited by B. Doucot and J. Zinn-Justin (Elsevier Science, Amsterdam, 1995), p. 307.
- [29] B. J. Klemme *et al.*, Phys. Rev. Lett. **75**, 2408 (1995).
 - [30] S. E. Brown *et al.*, Synthetic Metals **86**, 1937 (1997).
 - [31] V. Vescoli *et al.*, Science **281**, 1181 (1998).
 - [32] N. Cao, T. Timusk, and K. Bechgaard, J. Phys. I (France) **6**, 1719 (1996).
 - [33] T. Giamarchi, Physica **B230-232**, 975 (1997).
 - [34] M. T. Béal-Monod, C. Bourbonnais, and V. J. Emery, Phys. Rev. B **34**, 7716 (1986).
 - [35] J. Pouget *et al.*, Mol. Cryst. Liq. Cryst. **79**, 129 (1982).
 - [36] S. Barisic and S. Brazovskii, in *Recent Developments in Condensed Matter Physics*, edited by J. T. Devreese (Plenum, New York, 1981), Vol. 1, p. 327.
 - [37] C. Bourbonnais and B. Dumoulin, J. Phys. I (France) **6**, 1727 (1996).
 - [38] V. J. Emery, Synthetic Metals **13**, 21 (1986).
 - [39] W. Kohn and J. M. Luttinger, Phys. Rev. Lett. **15**, 524 (1965).
 - [40] B. Guay and C. Bourbonnais, Synthetic Metals **103**, 2180 (1999).
 - [41] L. G. Caron and C. Bourbonnais, Physica **143B**, 453 (1986).